


 Cite this: *Chem. Commun.*, 2019, 55, 5255

 Received 5th March 2019,
 Accepted 8th April 2019

DOI: 10.1039/c9cc01825e

rsc.li/chemcomm

Covalently functionalized carbon nanoparticles with a chiral Mn-Salen: a new nanocatalyst for enantioselective epoxidation of alkenes†

 Agatino Zammataro,^a Chiara Maria Antonietta Gangemi,^a Andrea Pappalardo,^{ab} Rosa Maria Toscano,^a Roberta Puglisi,^a Giuseppe Nicotra,^c Maria Elena Fragalà,^a Nunzio Tuccitto^{ad} and Giuseppe Trusso Sfrassetto^{ab*}

A new protocol to obtain carbon nanoparticles (CNPs) covalently functionalized with a chiral Mn-Salen catalyst is described here. The new nanocatalyst (CNPs-Mn-Salen) was tested in the enantioselective epoxidation of some representative alkenes (CN-chromene, 1,2-dihydronaphthalene and *cis*- β -ethyl styrene), obtaining better enantiomeric excess values than that of the catalyst single molecule, highlighting the role of the nanostructure in the enantioselectivity.

Olefin epoxidation is one of the most important and useful reactions due to the possibility of obtaining a wide range of organic derivatives. This reaction has found application in several technological fields.¹ In this context, chiral Mn(III)-Salen derivatives play a central role due to their huge employment in the synthesis of chiral epoxides, which represent an important target for pharmaceuticals and industry.^{2–4} However, exposure to transition metal ions, in particular manganese, at concentrations more than 5 $\mu\text{g m}^{-3}$, can lead to important neurological disorders.⁵ Therefore, many efforts have been devoted towards reducing the amount of this metal ion in catalytic systems. One of the most used strategies is to heterogenize Jacobsen's catalyst onto a solid surface.^{6–13} Another strategy is to obtain nanocatalysts¹⁴ in which the amount of metal atoms is significantly reduced compared to standard catalysts.

Carbon nanoparticles (CNPs) are a new class of carbon nanomaterials which exhibit interesting photo-chemical and redox properties.¹⁵ CNPs are nanoparticles about 10 nm in diameter, with a quasi-spherical shape. Due to their high optical and chemical stability, good water solubility, photobleaching resistance,

biocompatibility and low cost, nowadays CNPs are successfully applied to a wide range of application fields, such as analytical chemistry,^{16,17} biosensing,^{18,19} bioimaging,^{20,21} theranostics,^{22,23} molecular communication^{24,25} and photocatalytic energy conversion.^{26–28} However, very few examples of CNPs used as catalysts have been reported.^{29–37} Among them, no example of catalyst for epoxidation has been described.

Although the one pot synthesis of CNPs is green, simple and versatile, the obtained CNP derivatives do not display yet the properties achieved by covalent functionalization of their external shell. Attractive hybrid approaches that combine one-pot synthesis with covalent functionalization of the functional groups of the external shell may lead to a versatile and efficient preparation of new CNPs having different surface functionalities. Thus, decorating CNPs with a functional substrate/catalyst is a promising option to enhance their properties.

Here, the first example of covalent functionalization of CNPs with a chiral Mn-Salen catalyst (**Mn-Salen-OH**, Scheme 1) is reported. The Salen ligand has been functionalized in order to covalently react with carboxylic groups on the surfaces of the native CNPs, leading to the formation of an ester bond. The new nanostructure was tested as a catalyst for the enantioselective epoxidation of alkenes, by using 1,2-dihydronaphthalene, CN-chromene and *cis*- β -ethyl styrene as model substrates. Scheme 1 shows the synthetic pathway to obtain the **Mn-Salen-OH** catalyst. Salicylaldehyde was chloromethylated by using aqueous formaldehyde in hydrochloric acid, obtaining aldehyde **1** which, after reaction with CuSO_4 in $\text{DMSO}/\text{H}_2\text{O}$, was converted into 5-hydroxymethyl-2-hydroxy-benzaldehyde **2**.³⁸ The chiral Salen ligand **4** was obtained by reaction of **2** with (1*R*,2*R*)-diphenylethylenediamino-monochloride derivative **3**,^{39,40} in the presence of triethylamine. Then, manganese was introduced into the Salen ligand obtaining **Mn-Salen-OH** in almost quantitative yield.^{41,42} All new compounds have been characterized by NMR and ESI-MS (see the ESI†). The presence of the hydroxylic group on the Salen backbone allows anchoring of this catalyst onto the surfaces of the native CNPs. These, in fact, contain

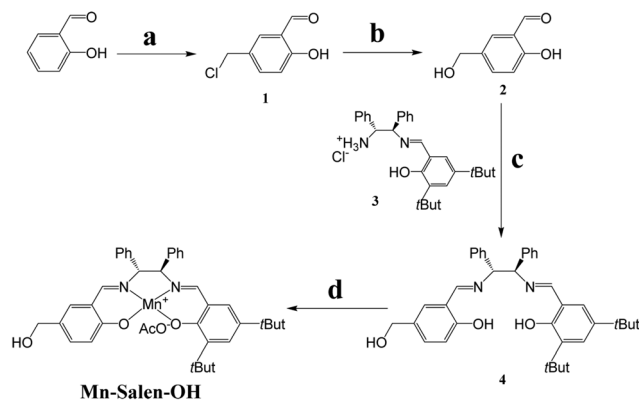
^a Department of Chemical Sciences, University of Catania, Viale Andrea Doria 6, 95125, Catania, Italy. E-mail: giuseppe.trusso@unicat.it

^b INSTM Udr of Catania, Viale Andrea Doria 6, 95125, Catania, Italy

^c CNR-IMM, Zona industriale strada VIII, 5, 95121 Catania, Italy

^d Laboratory for Molecular Surfaces and Nanotechnology (LAMSun), Department of Chemical Sciences, University of Catania and CSGI, Italy

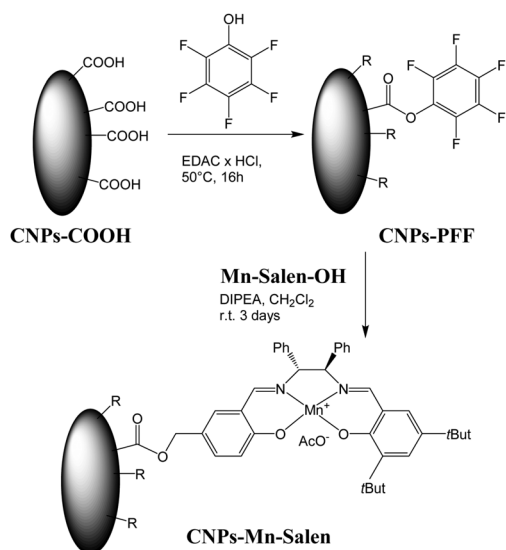
† Electronic supplementary information (ESI) available: Synthetic procedures, characterization of compounds, NMR, ESI-MS, XPS spectra, and SEM and TEM images. See DOI: 10.1039/c9cc01825e



Scheme 1 Synthesis of **Mn-Salen-OH**. Reagents and conditions: (a) formaldehyde (37% aqueous solution), concentrated HCl, 90 °C, 16 h, 85%; (b) CuSO₄, H₂O/DMSO (1/2), 110 °C, 2 h, 87%; (c) Et₃N, EtOH, RT, 16 h, 65%; and (d) Mn(OAc)₃, EtOH, RT, 16 h, 95%.

several free carboxylic groups on their surfaces which, after activation, can react with **Mn-Salen-OH**, leading to the formation of a stable covalent bond. Native CNPs were synthesized by hydrothermal decomposition.²⁴

The covalent functionalization of their surfaces is shown in Scheme 2. The carboxylic groups of the CNPs (**CNPs-COOH**) were activated by using pentafluorophenol and EDAC × HCl (*N*-(3-dimethylaminopropyl)-*N'*-ethylcarbodiimide hydrochloride) in solvolysis at 50 °C overnight. The functionalized CNPs (**CNPs-PFF**) were purified by extraction in water/dichloromethane, due to their higher solubility in organic solvent compared to the starting **CNPs-COOH**. Then, reaction of **CNPs-PFF** with a large excess of **Mn-Salen-OH** leads to the formation of the nanocatalyst **CNPs-Mn-Salen**, which was purified by dialysis. **CNPs-Mn-Salen** was characterized by ¹H NMR, XPS, TEM and SEM. In particular, its ¹H NMR spectrum shows broad signals, according to the presence of manganese metal ions, in the region relative to the Salen complex (see the ESI[†]).



Scheme 2 Functionalization of CNPs with chiral **Mn-Salen-OH**.

The XPS spectrum of the as prepared **CNPs-Mn-Salen** sample shows a C 1s band at 285.0 eV (Fig. S8, see ESI[†]), partially asymmetric due to the chemical shift of C 1s related to carboxylate species having a higher binding energy.

Fig. 1a shows the XPS Mn 2p_{3/2,1/2} spin-orbit components at 642.3 and 654.1 eV, partially overlapping with the high energy shake-up satellites typical of Mn(III) species,^{12,13,43,44} while the XPS spectrum of the O 1s states for the **CNPs-Mn-Salen** sample shows two evident signals at 532.5 and 530.2 eV (Fig. 1b). The first peak is largely due to the SiO₂ substrate, and the shoulder at a lower binding energy is assigned to the chemical shift related to the O–Mn and –COOH groups. Moreover, the XPS of the **CNPs-Mn-Salen** sample in the N 1s binding energy region exhibits a signal at 400.0 eV (Fig. 1c), since the Mn–Salen complex possesses two imine groups.^{12,13} Although XPS is a surface sensitive analytical technique, and since the diameter of the CNPs is smaller²⁴ than the sampling depth of the XPS, we were able to probe the whole CNP particle. Considering that the area of a **Mn-Salen** molecule is 1.4 nm²,¹³ we expect, in the case of complete surface coverage, 150 atoms of Mn per CNP having a diameter of 7 nm. The XPS C/Mn atomic concentration ratio is found to be 195, corresponding to 55 atoms of Mn per CNP matching with a coverage of 33%. Taking into account the well-known adventitious carbon contamination, omnipresent in all air-exposed materials, the coverage is satisfactory in view of the catalytic purpose of such organic nanostructures.

TEM analysis reveals the presence of nanoparticles having an average diameter of 8 nm (Fig. 2). Moreover, images taken at high resolution (HR-TEM, see the ESI,† Fig. S11) reveal the presence of graphite-like carbon crystal structures in the nanoparticles' cores. The external shell around the CNPs is even visible as a slightly dark contrast around the cores of the CNPs (inset of Fig. 2). This is compatible with the presence of the functionalized complex anchored onto the CNPs' surfaces. SEM analysis is in good agreement with TEM results. SEM images confirm the formation of carbon nanoparticles with dimensions ranging from a few nanometers (see the ESI,† Fig. S10 red arrows) to 20–40 nm. However, particle aggregation on the substrate cannot be excluded during solvent evaporation.

Preliminary epoxidation results by using **CNPs-Mn-Salen** are shown in Table 1.

1,2-Dihydronaphthalene was chosen as the substrate to set up the epoxidation conditions. In particular, by using a nanocatalyst concentration of 0.05 mg mL^{−1}, good enantiomeric

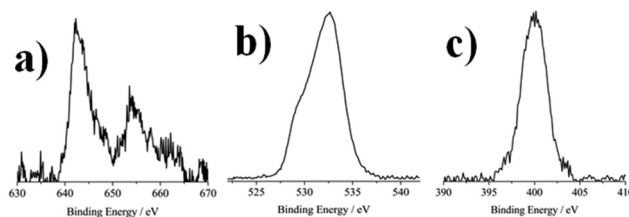


Fig. 1 Al K α excited XPS of the CNP sample, measured in the (a) Mn 2p, (b) O 1s and (c) N 1s binding energy regions. The structure due to satellite radiation has been subtracted from the spectra.

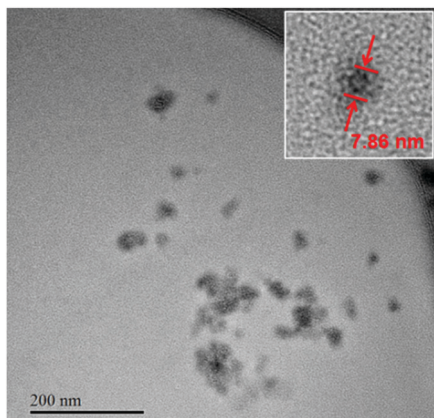
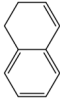
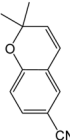
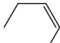


Fig. 2 BF-TEM image acquired at 200 keV at a low e^- dose shows the presence of small CNPs with an average size of 8 nm.

excesses but low conversion values were obtained (Table 1, entries 1–3). By increasing the concentration of **CNPs-Mn-Salen** (0.5 mg mL^{-1}) the conversion values increased (Table 1, entries 4–6). This setup was used with CN-chromene (Table 1, entries 7–9) and *cis*- β -ethyl styrene (Table 1, entries 10–12). In particular, with CN-chromene, the conversion values were lower than those obtained with 1,2-dihydronaphthalene, but the enantiomeric excess values were 95–96%, higher than those obtained with **Mn-Salen-OH** (see control reactions in Table 1). These results suggest that the presence of CNPs increases the enantiomeric excess, in the case of CN-chromene, although the conversion is low. The origin of the high enantioselectivity in Jacobsen's epoxidation has been extensively studied,⁴⁶ but, until now, not fully elucidated. The most common rationalization is attributed to the directions of approach of the alkene to the manganese active site (manganese-oxo). Cavallo and co-workers reported theoretical calculations that support this hypothesis.⁴⁷ More recently, a new justification about the origin of the enantioselectivity was proposed by Corey and coworkers.⁴⁸ In this hypothesis, the transition state assembly is slightly similar to a [3+2] cycloaddition between the alkene and the catalyst. A possible explanation for the high enantioselectivity with CN-chromene can be ascribed to the chemical structure of this alkene. In particular, due to the presence of an oxygen atom in the fused ring system, some possible interactions can occur with the surfaces of the CNPs (e.g. H-bonding with some unfunctionalized groups) that decrease the reactivity, leading to low conversion values but, at the same time, increase the geometric constraints, thus resulting in high enantiomeric excess values.

Epoxidation reactions with *cis*- β -ethyl styrene showed good conversion values after 1 hour (59%, Table 1, entry 10), higher than those of the other examined alkenes. This higher reactivity led to lower enantiomeric excess values ($\sim 71\%$, Table 1, entries 10–12) than those of the other substrates, as well as that of **Mn-Salen-OH** (Table 1, entry 13).² Furthermore, the [*cis*]/[*trans*] ratio (~ 7 , with $\sim 50\%$ ee values) suggests a short lifetime of the radical intermediate, invoked by Jacobsen and co-workers,⁴⁹ leading to the partial isomerization of the radical intermediate.

Table 1 Enantioselective epoxidation of 1,2-dihydronaphthalene, 6-CN-2,2-dimethylchromene and *cis*- β -ethyl styrene with NaClO catalyzed by **CNPs-Mn-Salen** in CH_2Cl_2 at 25°C ^a

Alkene	Entry	Nanocat. (mg mL ⁻¹) ^b	Time (h)	ee ^c (%)	Conv. ^c (%)	TON ^f (TOF) ^g	CB ^h (%)
	1	0.05	1	80 ^d	10	8264 (8264)	97
	2	0.05	12	81 ^d	12	9917 (4959)	95
	3	0.05	24	80 ^d	15	12 397 (1033)	94
	4	0.5	1	79 ^d	35	2893 (2893)	95
	5	0.5	12	80 ^d	49	4050 (337)	93
	6	0.5	24	80 ^d (82) ^j	50 (100) ^j	4132 (172)	92 (97) ^j
	7	0.5	1	96 ^e	18	1488 (1488)	96
	8	0.5	12	96 ^e	29	2397 (200)	94
	9	0.5	24	95 ^e (75) ^j	30 (100) ^j	2479 (103)	94 (96) ^j
Alkene	Entry	Time (h)	ee ^{cis} ee ^{trans} ^c (%)	<i>cis</i> / <i>trans</i>	Conv. ^c (%)	TON ^f (TOF) ^g	CB ^h (%)
	10 ⁱ	1	71 ^d 52 ^d	7	59	4876 (4876)	97
	11 ⁱ	12	71 ^d 50 ^d	7	65	5372 (448)	95
	12 ⁱ	24	72 ^d 50 ^d	7	66	5455 (227)	95
	13 ^j	24	85 ^d 59 ^d	5	100	1176 (49)	97

^a In all experiments [alkene] = [NaClO] = $1.17 \times 10^{-2} \text{ M}$, buffered with 1 mL of $0.05 \text{ M Na}_2\text{HPO}_4$ at pH 11.2 in a total volume of 2 mL. ^b A stock solution of **CNPs-Mn-Salen** was prepared dissolving 5 mg of nanocatalyst in 5 mL of CH_2Cl_2 . ^c Determined by GC analysis using a chiral column (see the ESI) and *n*-dodecane as an internal standard. ^d Config. (1*R*,2*R*) determined by measuring the optical rotation. ^e Config. (3*R*,4*R*) determined by measuring the optical rotation. ^f TON = [overall products]/[catalyst]. ^g TOF = TON/reaction time (h). ^h Carbon balance CB = (total carbon detected/total carbon feed).⁴⁵ ⁱ [**CNPs-Mn-Salen**] = 0.5 mg mL^{-1} . ^j Control reaction was performed by using [**Mn-Salen-OH**] = $8.50 \times 10^{-4} \text{ M}$, and [alkene] = [NaClO] = $1.17 \times 10^{-2} \text{ M}$, buffered with 1 mL of $0.05 \text{ M Na}_2\text{HPO}_4$ at pH 11.2 in a total volume of 2 mL. With 1,2-dihydronaphthalene as the substrate, after 24 h, total conversion and 82% enantiomeric excess were obtained. With CN-chromene as the substrate, after 24 h, total conversion and 75% enantiomeric excess were obtained. With *cis*- β -ethyl styrene as the substrate, after 24 h, total conversion and 85% enantiomeric excess were obtained.

Recycling tests were performed by using 1,2-dihydronaphthalene as the selected substrate (see the ESI,† Fig. S9). **CNPs-Mn-Salen** can be recovered from the reaction media by extraction with CH_2Cl_2 (to remove the aqueous phase), and vacuum treatment at 100°C for two hours (to remove the organic products/byproducts). After 4 cycles, the enantiomeric excesses remained almost unaltered, while the conversion values decreased from 50% to 25%, suggesting a partial degradation of the nanocatalyst.

In summary, a new synthetic protocol for the covalent functionalization of CNPs was reported. In particular, we anchored a chiral Mn-Salen catalyst onto CNPs, leading to a new nanocatalyst able to catalyze the enantioselective epoxidation of some selected alkenes. This new catalytic system, using CN-chromene as the

substrate, allows chiral epoxides with higher enantiomeric excess values than that with the molecular catalyst to be obtained. We are still testing this nanocatalyst with other substrates in order to shed light on the origin of this enantioselectivity. Preliminary results revealed that the role of the nanostructure is essential in increasing the enantioselectivity. Compared to commercial catalysts used for the oxidation of organic substrates,⁵⁰ chiral Mn-Salen allows control over the enantioselectivity of the reaction. Furthermore, the functionalization of carbon materials with Mn-Salen catalysts allows the amount of Mn in the reaction media to be reduced and, in addition, an improvement in the stability of these nanocatalysts under alkaline conditions, which requires the presence of NaClO as the oxidant. Basic conditions, in fact, are harmful for silica supports, which are largely used for the heterogenization of Jacobsen's catalysts.

The authors thank Prof. Antonino Gulino and Dr Luca Spitaleri for XPS measurements. This work was supported by the University of Catania, Department of Chemical Sciences (Piano per la Ricerca 2016-2018-Linea Intervento 2).

Conflicts of interest

There are no conflicts to declare.

Notes and references

- C. Baleizão, *Chem. Rev.*, 2006, **106**, 3987–4043.
- E. N. Jacobsen, *Catalytic Asymmetric Synthesis*, ed. I. Ojima, VCH, Weinheim, Germany, 1993, ch. 4.2, pp. 159–202.
- T. P. Yoon and E. N. Jacobsen, *Science*, 2003, **299**, 1691–1693.
- I. W. E. E. Arends, *Angew. Chem., Int. Ed.*, 2006, **45**, 6250–6252.
- R. M. Bowler, S. Nakagawa, M. Drezgic, H. A. Roels, R. M. Park, E. Diamond, D. Mergler, M. Bouchard, R. P. Bowler and W. Koller, *Neurotoxicology*, 2007, **28**, 298–311.
- J. M. Thomas and R. Raja, *Acc. Chem. Res.*, 2008, **41**, 708–720.
- J. R. Carey, S. K. Ma, T. D. Pfister, D. K. Garner, H. K. Kim, J. A. Abramite, Z. Wang, Z. Guo and Y. Lu, *J. Am. Chem. Soc.*, 2004, **126**, 10812–10813.
- M. Pala and V. Ganesan, *Catal. Sci. Technol.*, 2012, **2**, 2383–2388.
- R. Raja, J. M. Thomas, M. D. Jones, B. F. G. Johnson and D. E. W. Vaughan, *J. Am. Chem. Soc.*, 2003, **125**, 14982–14983.
- C. Bianchini and P. Barbaro, *Top. Catal.*, 2002, **19**, 17–32.
- J. M. Fraile, J. I. Garcia, C. I. Herrerias, J. A. Mayoral and E. Pires, *Chem. Soc. Rev.*, 2009, **38**, 695–706.
- V. La Paglia Fragola, F. Lupo, A. Pappalardo, G. Trusso Sfrazzetto, R. M. Toscano, F. P. Ballistreri, G. Tomaselli and A. Gulino, *J. Mater. Chem.*, 2012, **22**, 20561–20565.
- G. Trusso Sfrazzetto, S. Millesi, A. Pappalardo, R. M. Toscano, F. P. Ballistreri, G. A. Tomaselli and A. Gulino, *Catal. Sci. Technol.*, 2015, **5**, 673–679.
- A. Agnoli, *Eur. J. Inorg. Chem.*, 2018, 4311–4321.
- F. R. Baptista, S. A. Belhout, S. Giordani and S. J. Quinn, *Chem. Soc. Rev.*, 2015, **44**, 4433–4453.
- Y. M. Guo, Z. Wang, H. W. Shao and X. Y. Jiang, *Carbon*, 2013, **52**, 583–589.
- S. N. Qu, H. Chen, X. M. Zheng, J. S. Cao and X. Y. Liu, *Nanoscale*, 2013, **5**, 5514–5518.
- W. Shi, X. Li and H. Ma, *Angew. Chem., Int. Ed.*, 2012, **51**, 6432–6435.
- A. W. Zhu, Q. Qu, X. L. Shao, B. Kong and Y. Tian, *Angew. Chem., Int. Ed.*, 2012, **51**, 7185–7189.
- S. T. Yang, L. Cao, P. J. G. Luo, F. S. Lu, X. Wang, H. F. Wang, M. J. Mezziani, Y. F. Liu, G. Qi and Y. P. Sun, *J. Am. Chem. Soc.*, 2009, **131**, 11308–11309.
- N. Licciardello, S. Hunoldt, R. Bergmann, G. Singh, C. Mamat, A. Faramus, J. L. Z. Ddungu, S. Silvestrini, M. Maggini, L. De Cola and H. Stephan, *Nanoscale*, 2018, **10**, 9880–9891.
- L. Hu, Y. Sun, S. Li, X. Wang, K. Hu, L. Wang, X.-J. Liang and Y. Wu, *Carbon*, 2014, **67**, 508–513.
- H. Wang, G. Cao, Z. Gai, K. Hong, P. Banerjee and S. Zhou, *Nanoscale*, 2015, **7**, 7885–7895.
- N. Tuccitto, G. Li-Destri, G. M. L. Messina and G. Marletta, *J. Phys. Chem. Lett.*, 2017, **8**, 3861–3866.
- N. Tuccitto, G. Li-Destri, G. M. L. Messina and G. Marletta, *Phys. Chem. Chem. Phys.*, 2018, **20**, 30312–30320.
- V. Strauss, J. T. Margraf, C. Dolle, B. Butz, T. J. Nacken, J. Walter, W. Bauer, W. Peukert, E. Spiecker, T. Clark and D. M. Guldi, *J. Am. Chem. Soc.*, 2014, **136**, 17308–17316.
- W. Tu, Y. Zhou and Z. Zou, *Adv. Mater.*, 2014, **26**, 4607–4626.
- S. N. Habisreutinger, L. Schmidt-Mende and J. K. Stolarczyk, *Angew. Chem., Int. Ed.*, 2013, **52**, 7372–7408.
- L.-M. Shen and J. Liu, *Talanta*, 2016, **156–157**, 245–256.
- S. Muthulingam, I.-H. Lee and P. Uthirakumar, *J. Colloid Interface Sci.*, 2015, **455**, 101–109.
- B. C. M. Martindale, G. A. M. Hutton, C. A. Caputo and E. Reisner, *J. Am. Chem. Soc.*, 2015, **137**, 6018–6025.
- J. Briscoe, A. Marinovic, M. Sevilla, S. Dunn and M. Titirici, *Angew. Chem., Int. Ed.*, 2015, **54**, 4463–4468.
- H. Li, C. Sun, M. Ali, F. Zhou, X. Zhang and D. R. MacFarlane, *Angew. Chem., Int. Ed.*, 2015, **54**, 8420–8424.
- D. Mosconi, D. Mazzier, S. Silvestrini, A. Privitera and C. Marega, *ACS Nano*, 2015, **9**, 4156–4164.
- S. Zhao, C. Li, J. Liu, N. Liu, S. Qiao, Y. Han, H. Huang, Y. Liu and Z. Kang, *Carbon*, 2015, **92**, 64–73.
- J.-J. Zhang, Z.-B. Wang, C. Li, L. Zhao, J. Liu, L.-M. Zhang and D.-M. Gu, *J. Power Sources*, 2015, **289**, 63–70.
- Y. Jin, C. Hu, Q. Dai, Y. Xiao, Y. Lin, J. W. Connell, F. Chen and L. Dai, *Adv. Funct. Mater.*, 2018, **28**, 1804630–1804637.
- A. Gulino, G. Trusso Sfrazzetto, S. Millesi, A. Pappalardo, G. A. Tomaselli, F. P. Ballistreri, R. M. Toscano and L. Fragalà, *Chem. – Eur. J.*, 2017, **23**, 1576–1583.
- A. Pappalardo, M. E. Amato, F. P. Ballistreri, G. A. Tomaselli, R. M. Toscano and G. Trusso Sfrazzetto, *J. Org. Chem.*, 2012, **77**, 7684–7687.
- A. D'Urso, C. Tudisco, F. P. Ballistreri, G. G. Condorelli, R. Randazzo, G. A. Tomaselli, R. M. Toscano, G. Trusso Sfrazzetto and A. Pappalardo, *Chem. Commun.*, 2014, **50**, 4993–4996.
- F. P. Ballistreri, C. M. A. Gangemi, A. Pappalardo, G. A. Tomaselli, R. M. Toscano and G. Trusso Sfrazzetto, *Int. J. Mol. Sci.*, 2016, **17**, 1112–1120.
- A. Patti, S. Pedotti, F. P. Ballistreri and G. Trusso Sfrazzetto, *Molecules*, 2009, **14**, 4312–4325.
- D. Q. Li, B. I. Swanson, J. M. Robinson and M. A. Hoffbauer, *J. Am. Chem. Soc.*, 1993, **115**, 6975–6980.
- M. C. Biesinger, B. P. Payne, A. P. Grosvenor, L. W. M. Lau, A. R. Gerson and R. S. C. Smart, *Appl. Surf. Sci.*, 2011, **257**, 2717–2730.
- M. S. C. Chan, E. Marek, S. A. Scott and J. S. Dennis, *J. Catal.*, 2018, **359**, 1–7.
- T. Katsuki, *Coord. Chem. Rev.*, 1995, **140**, 189–214.
- H. Jacobsen and L. Cavallo, *Chem. – Eur. J.*, 2001, **7**, 800–807.
- L. Kurti, M. M. Blewett and E. J. Corey, *Org. Lett.*, 2009, **11**, 4592–4595.
- W. Zhang, N. H. Lee and E. N. Jacobsen, *J. Am. Chem. Soc.*, 1994, **116**, 425–426.
- R. A. F. Tomás, J. C. M. Bordado and J. F. P. Gomes, *Chem. Rev.*, 2013, **113**, 7421–7469.